CHAPTER 3

Results and discussion

In this research, calcium peroxide (CaO_2) powders were synthesized by a co-precipitation method with various synthetic conditions, for example; precursors variation, H_2O_2 addition rate variation, precipitating agents variation, drying temperatures. In addition, this research also studied the effect of some additive as chelator-controlled nanoparticle such as ethanol, Triton-X and ascorbic acid. The synthesized CaO_2 powders were then characterized by XRD, SEM, TEM and BET techniques to find an optimum condition for a productive method to synthesize high-purity nanoparticle CaO_2.

3.1 Characterization of the powders synthesized by different precursors.

In this research, researcher studied effect of precursor. There are several calcium precursor can be used for synthesis of CaO_2, which may lead to a significant difference of physical and chemical properties. This work has selected $CaCO_3$, $Ca(OH)_2$, $CaCl_2$ and $Ca(NO_3)_2$ as precursors under the same condition for comparison. Dissolution of $CaCO_3$ and $Ca(OH)_2$ in HNO_3 solution is required before using as precursors because they are insoluble in water. Whereas, $CaCl_2$ and $Ca(NO_3)_2$ can be easily dissolved in water. XRD patterns of CaO_2 powders prepared using several precursors such as $CaCO_3$, $Ca(OH)_2$, $CaCl_2$ and $Ca(NO_3)_2$ characterization by (Rigaku Mini Flex II are shown in (Fig. 3.1). It was found that phase and intensity of major peaks are CaO_2, which have 6 main peaks at 2θ = 30.3°, 35.6°, 47.3°, 51.6°, 53.2° and 60.9° (JCPDS card number 00-003-0865). However, there are some minor peaks of $CaCO_3$ at 2θ = 23.0°, 29.4°, 36.0°, 39.5°, 43.2°, 47.3°, 48.6°; 57.6° and 61.3° (JCPDS card number 00-001-0837), depending on the precursor. Fig. 5A shows XRD spectrum of powder synthesized using $CaCO_3$ as a precursor. It was found that a major phase is $CaCO_3$ and

no CaO_2 peak was observed. Fig 5B, 5C and 5D show peak of the powders synthesized using $Ca(OH)_2$, $CaCl_2$, and $Ca(NO_3)_2$, respectively. Major phase of CaO_2 and minor phase of $CaCO_3$ were observed. Therefore, $Ca(NO_3)_2$ would be good for synthesis of high purity CaO_2 nanoparticle in mild condition because there was small amount of minor phase at 2θ = 29.4° ($CaCO_3$) compared with other precursors. Moreover, $Ca(NO_3)_2$ is inexpensive, endothermic reaction when using peroxide based route, which is different from exothermic reaction when using other precursors. As a result, $Ca(NO_3)_2$ is chosen to be precursor for further investigation.

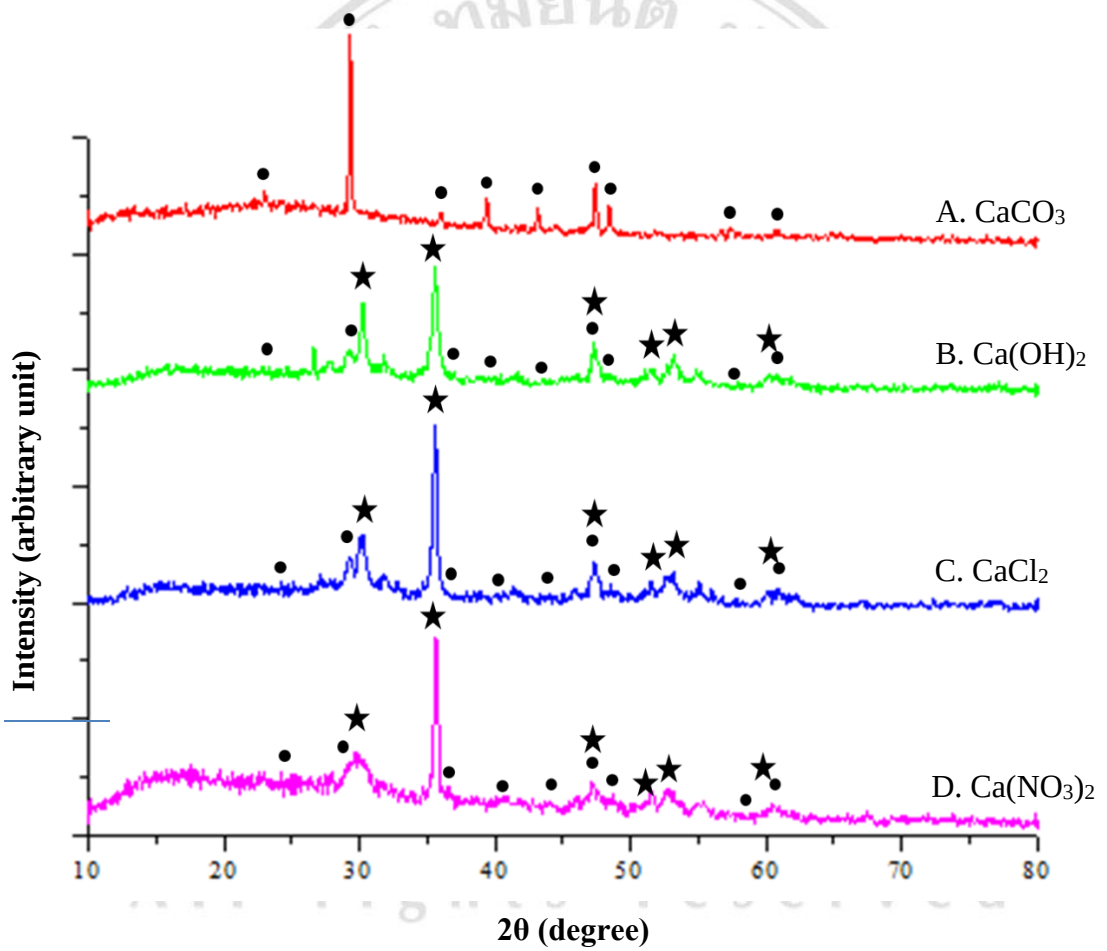

★ CaO_2 JCPDS No.00-003-0865 ● $CaCO_3$ (Calcite) JCPDS No. 00-001-0837

Figure 5. XRD patterns of CaO_2 powders prepared using several precursors e.g. $CaCO_3$, $Ca(OH)_2$, $CaCl_2$ and $Ca(NO_3)_2$.

3.2 Characterization of the powders synthesized by different H_2O_2 additional rate

In order to increase purity of CaO_2 prepared using $Ca(NO_3)_2$ as precursor by removing $CaCO_3$ impurity, other factors to prevent a forming of $CaCO_3$ were studied. H_2O_2 dropping rate during forming CaO_2 may affect an interaction between calcium ion and peroxide ion and may affect the growth of nuclei of CaO_2 so that rapidly and slowly H_2O_2 drop wise were investigated. Comparison of H_2O_2 additional rate was done by slowly drop H_2O_2 30 ml into solution by using burette 3 drops/min, whereas, fast addition was done by transferring H_2O_2 from beaker rapidly at room temperature.

Fig 6. showed XRD spectra of the powder obtained by the effect of rate of H_2O_2 addition. It was found that the faster addition of H_2O_2, the lesser $CaCO_3$ forming. Higher purity CaO_2 phase, which have 6 main peaks at 2θ = 30.3°, 35.6°, 47.3°, 51.6°, 53.2° and 60.9° (JCPDS card number 00- 003-0865) and have a small minor phase of $CaCO_3$ at 2θ = 23.0°, 29.4°, 36.0°, 39.5°, 43.2°, 47.3°, 48.6°; 57.6° and 61.3° (JCPDS card number 00-001-0837) was observed in Fig 6B. While, slowly adding H_2O_2 caused only $CaCO_3$ (vaterite) phase as the major phase at 2θ = 20.7°, 22.8°, 24.8°, 27.0°, 29.4°, 32.8°, 35.7°, 39.1°, 45.5°, 47.0°, 48.6°, 52.6°, 55.7°, 60.0°, and 62.7° (JCPDS No.00-001-0132) as shown in Fig 6A. Slowly adding H_2O_2 may allow time for interaction between calcium ion and CO_2 gas in air, whereas, fast addition may prevent the CO_2 penetrating into the solution because there are some bubble gas rising, probably an oxygen gas, during adding H_2O_2. Therefore, fast rate of H_2O_2 adding is using throughout this work.

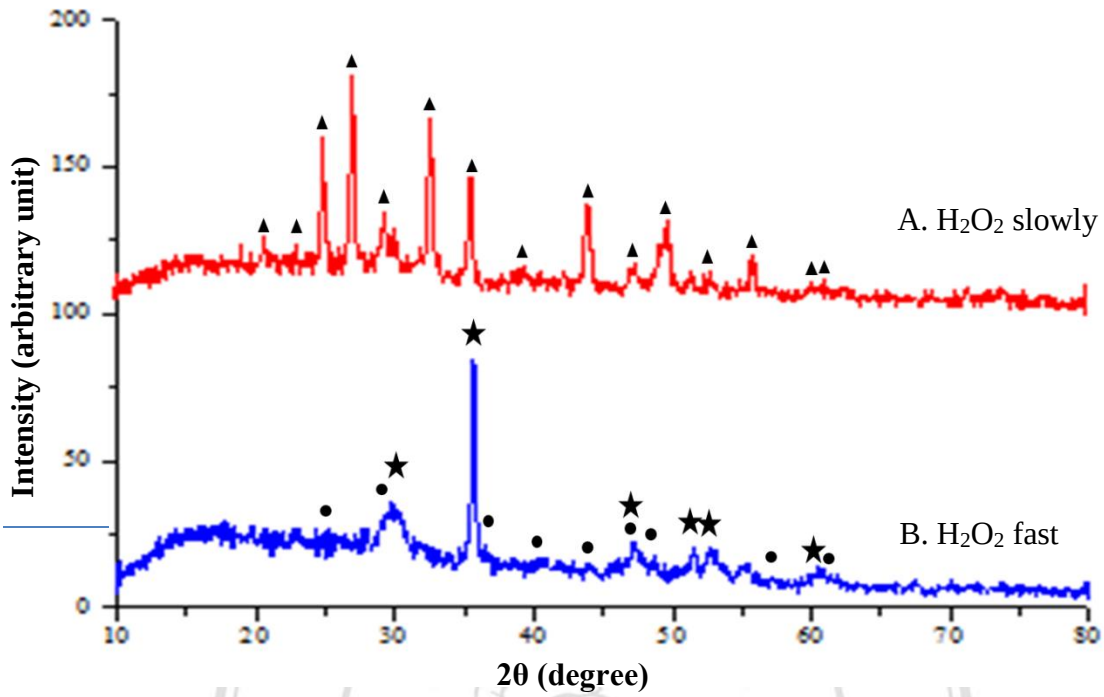

★ CaO_2 JCPDS No.00-003-0865 ●$CaCO_3$ (Calcite) JCPDS No. 00-001-0837

▲ $CaCO_3$ (vaterite) JCPDS No.00-001-0132

Figure 6. XRD patterns of powders obtained by the effect of rate of H_2O_2 addition

3.3 Characterization of the powders precipitated by NaOH and NH_4OH

Precipitating agent using NH_4OH and NaOH solution at pH 10 have been compared. Fig 7. showed XRD spectra of powders precipitated by NaOH and NH_4OH. Major phase CaO_2 with small minor phase $CaCO_3$ was obtained when using NH_4OH as reported earlier, as a result, NaOH was validated, expecting to decrease $CaCO_3$. However, minor phase $Ca(OH)_2$ peak at 2θ =18.0°, 28.7°,34.1°,47.1°, 54.4°, 59.4° and 62.6° (JCPDS No.00-044-1481) was obtained as another extra phase. This contaminate of product did not reduce $CaCO_3$ phase but, contrary, reduce intensity of CaO_2. This might be because hydroxide group of NaOH is stronger basicity than NH_4OH.

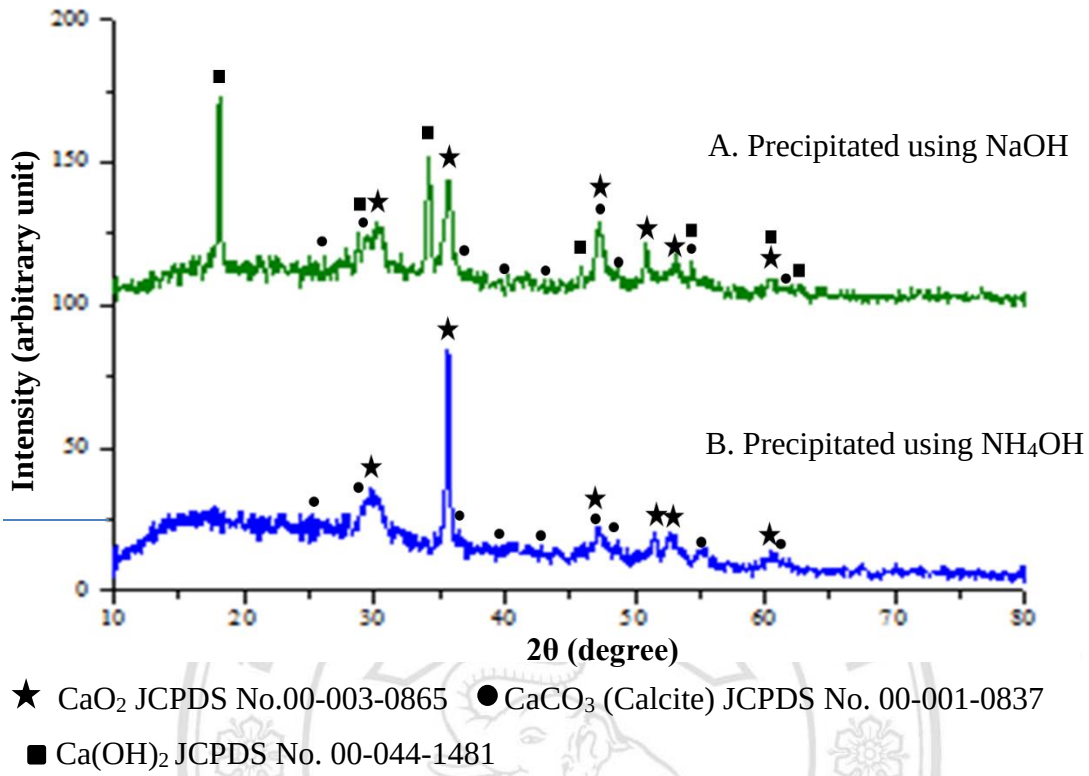

Figure 7. XRD patterns of powders precipitated by NaOH and NH_4OH

3.4 Characterization of the powders after washing by acetone, NH_4OH and distilled water

Washing precipitated powders would be an important step for pure phase of CaO_2 achievement because CaO_2 powders may have opportunity to contact with CO_2 in the air causing $CaCO_3$ contaminate in product during filtering. Therefore, 3 types of solution, which are acetone, NH_4OH and distilled water have been studied for powders washing. After major phase CaO_2 with small minor phase $CaCO_3$ was obtained by suitable starting material as mention earlier, washing with different solutions showed interesting effect as can be seen by XRD spectra in Fig 8. It was found that using NH_4OH would help to decrease the minor phase of $CaCO_3$ at $2\theta = 29.4°$ ($CaCO_3$ peak) (Fig 8B).

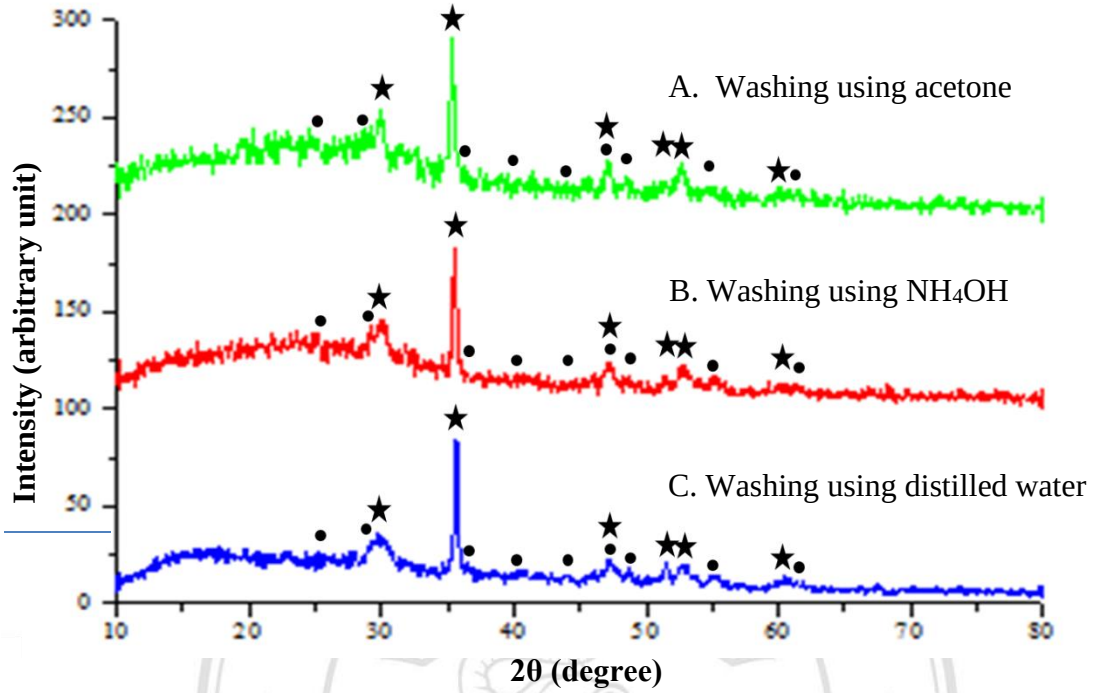

★ CaO_2 JCPDS No.00-003-0865 ● $CaCO_3$ (Calcite) JCPDS No. 00-001-0837

Figure 8. XRD patterns of powders washing with different solutions

3.5 Characterization of the powders after drying at various temperatures.

Final step of CaO_2 preparation that may also affect its purity is drying temperature. This work studied an effect of drying temperature at 80ºC, 150ºC and 200ºC. Knowing drying temperature tolerance of CaO_2 powders will provide important information for application. XRD patterns of CaO_2 powders after drying at 80°C, 150°C and 200°C showed some different phases as shown in Fig 9. Increasing drying temperature seems to induce extra phase of $CaCO_3$ phase at 2θ = 23.0°, 29.4°, 36.0°, 39.5°, 43.2°, 47.3°, 48.6°; 57.6°, 61.3° (JCPDS card number 00-001-0837) and Ca(OH)2 at 2θ =18.0°, 28.7° and 34.1°(JCPDS No. 00-044-1481). As a result, higher purity of CaO_2 can be obtained at lower drying temperature. However, CaO_2 is stable with remaining a major phase even drying at 150°C and 200°C, which have some small extra phase of $Ca(OH)_2$. It is noted that $Ca(OH)_2$ will be occurred at higher drying temperature instead of an increasing of $CaCO_3$.

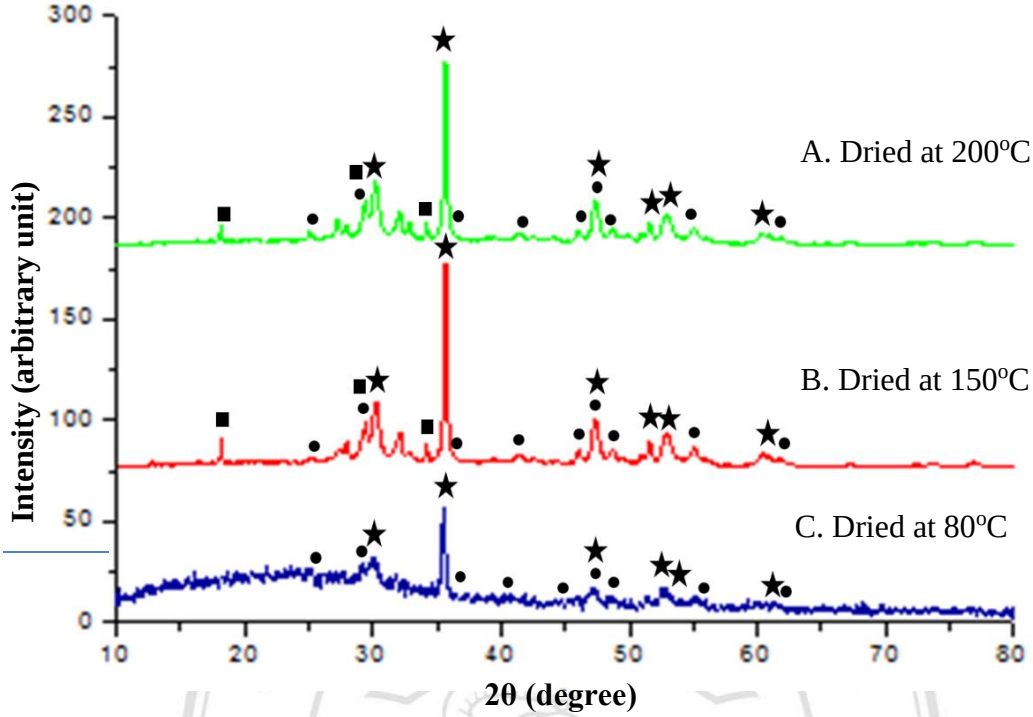

Figure 9. XRD patterns of CaO_2 powders after drying at 80°C, 150°C and 200°C showed some different phases.

3.6 Characterization of the powders synthesized with different additives

As nanoparticle may increase chemical properties or catalytic activities of CaO_2 because of surface area increment, reduction of particle has been attempted in this work. Previously, adding PEG-200 has been proposed as an impact factor for synthesis of nanoparticle of CaO_2. In this research, some additives were added in order to investigate the effect on controllable size of CaO_2 powders. Triton-X, ethanol and ascorbic acid additives were chosen for particle size comparison.

Preliminary results from XRD spectra of synthesized CaO_2 with additives such as Triton-X, Ethanol and Ascorbic acid are shown in Fig 10. It was found that additives did not affect to purity of CaO_2 as can be seen that no extra phase can be observed for all additives. On the other hand, higher purity was obtained when adding ethanol (Fig 10B.) lower vapor pressure of ethanol solution spread around particle and help to

protect CO_2 in the air reacted with CaO_2 causing $CaCO_3$. In addition, ethanol solution can easily eliminated by drying in oven at 80°C.

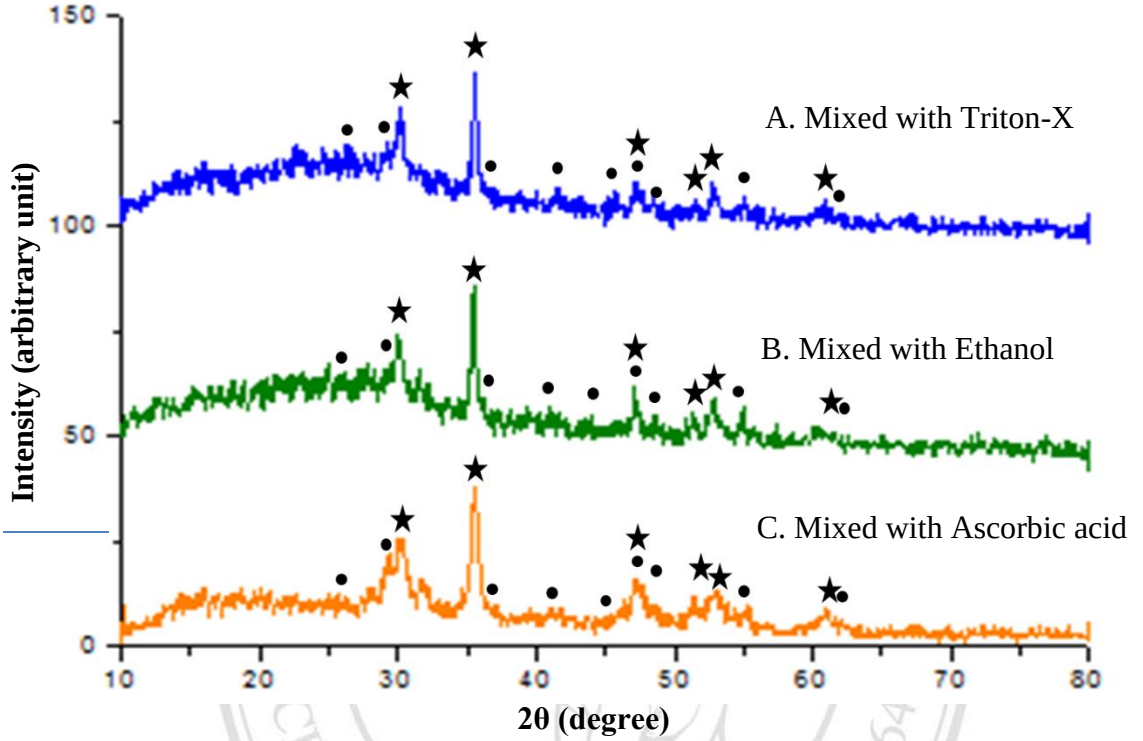

★CaO_2 JCPDS No.00-003-0865 ●$CaCO_3$ (Calcite) JCPDS No. 00-001-0837

Figure 10. XRD patterns of synthesized CaO_2 with additives such as Triton-X, ethanol and Ascorbic acid

3.7 Characterization of the CaO_2 powders by Scanning electron microscope (SEM)

SEM images of CaO_2 powders synthesized using $Ca(NO_3)_2$ after calcination at 80°C and 200°C are shown in Fig 11. and Fig 12.

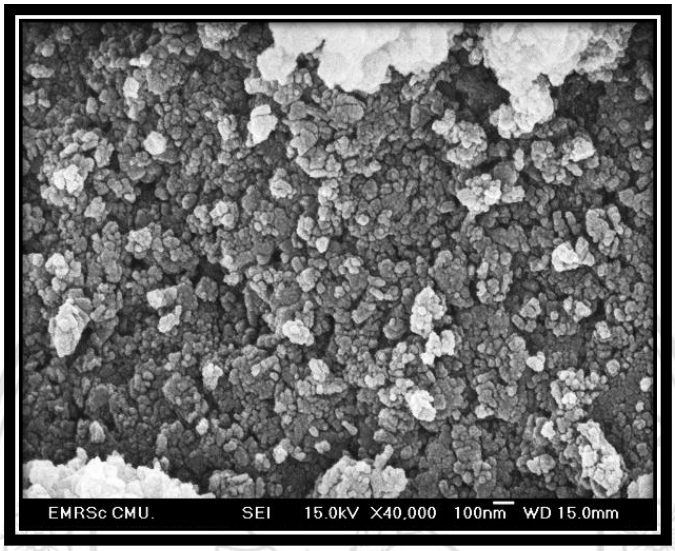

Figure 11. SEM images of CaO_2 powders synthesized using $Ca(NO_3)_2$ after calcination at 80°C 2 hr.

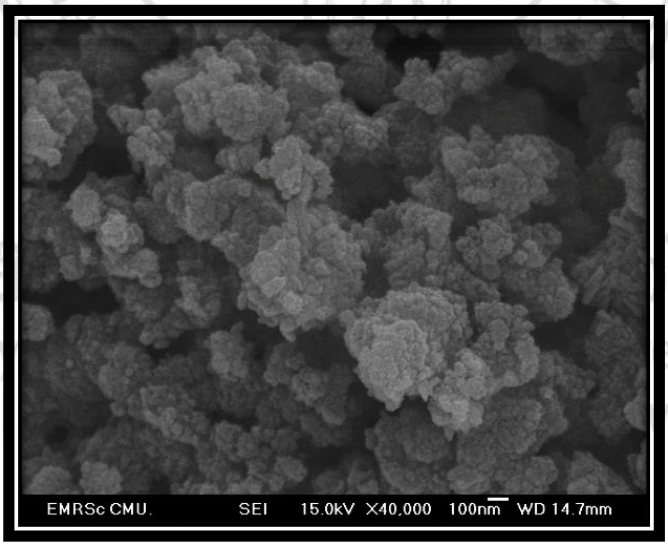

Figure 12. SEM images of CaO_2 powders synthesized using $Ca(NO_3)_2$ after calcination at 200°C 2 hr.

Low temperature drying at 80°C seems to provide more distribution of spherical particle of CaO_2 and showed small particle size, approximately 10-20 nm measuring by

Image J program. It is noted that CaO_2 prepared using $Ca(NO_3)_2$ as precursor can produce a smaller particle than using some conventional precursors $CaCl_2$ or $Ca(OH)_2$ in previous researches[24]. However, when drying high temperature CaO_2 particle tend to be more agglomerate.

Moreover, dwelling time of calcination at 200 ^oC between 2 hours and 6 hours was also compared.

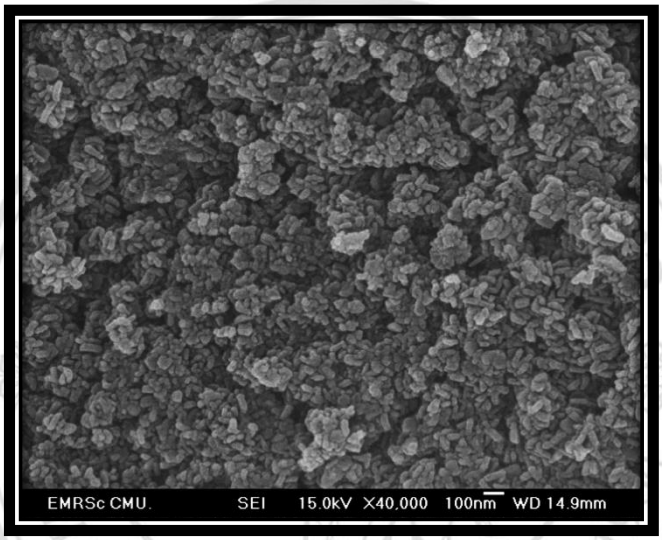

Figure 13. SEM images of CaO_2 powders after calcination at 200^oC 6 hr in magnification of 40,000x.

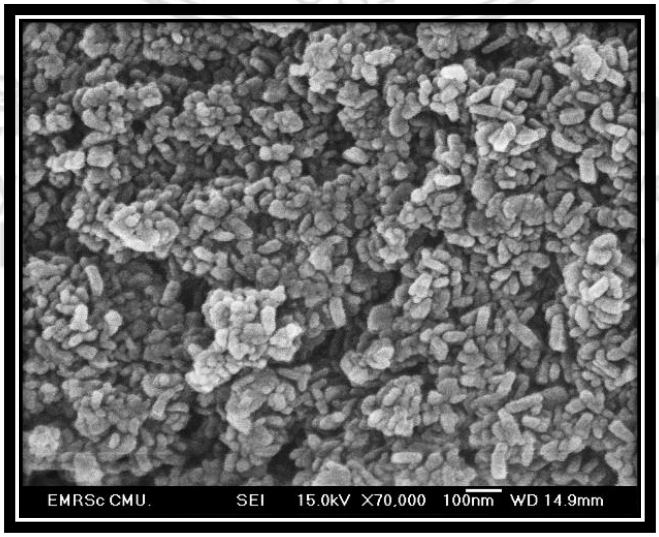

Figure 14. SEM images of CaO_2 powders after calcination at 200^oC 6 hr in magnification of 70,000x.

Interestingly, particle shape of the powders after drying at 200ºC for 6 hours was different from 2 hrs. Transforming from some spherical to rod shape, approximately 80-100 nm in length, can be observed and also higher distribution as can be seen in Fig 13. and Fig 14.

High purity of CaO_2 powders can be controlled after investigation as reported above so that morphology will be carried out when using various additives.

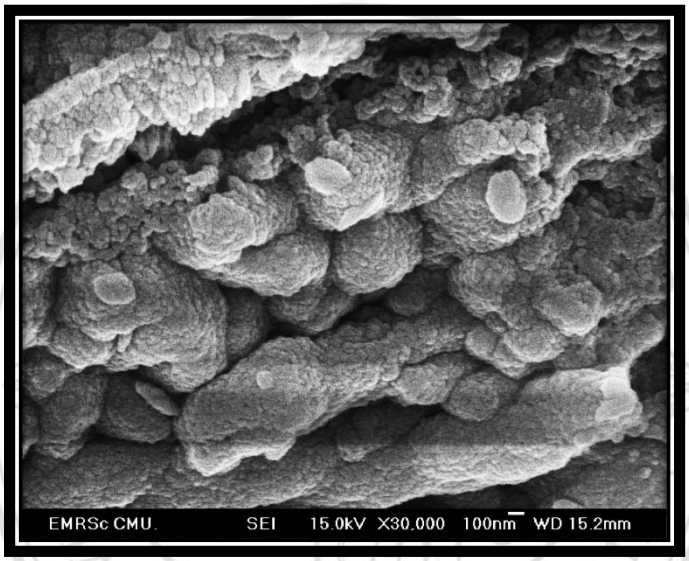

Figure 15. SEM images of CaO_2 powders in ethanol 1.

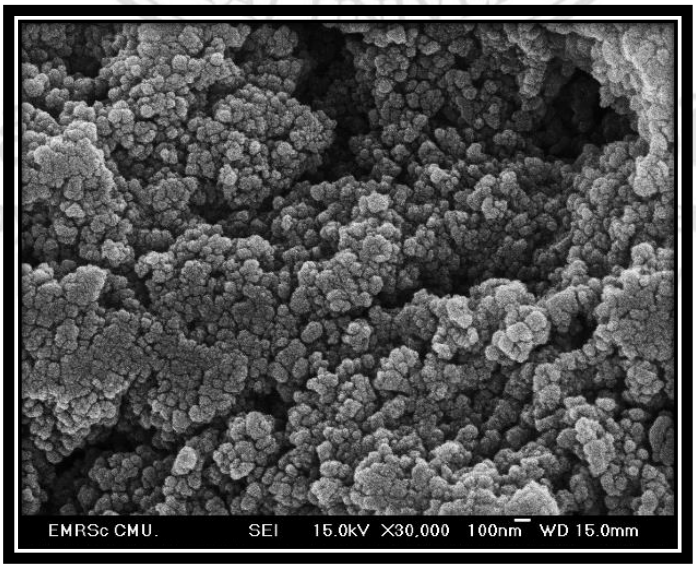

Figure 16. SEM images of CaO_2 powders in ethanol 2.

Ethanol additive leading to some bulk particles obtained from small particle agglomeration with some dispersion of nanosized particle as shown in Fig 15. and Fig 16.

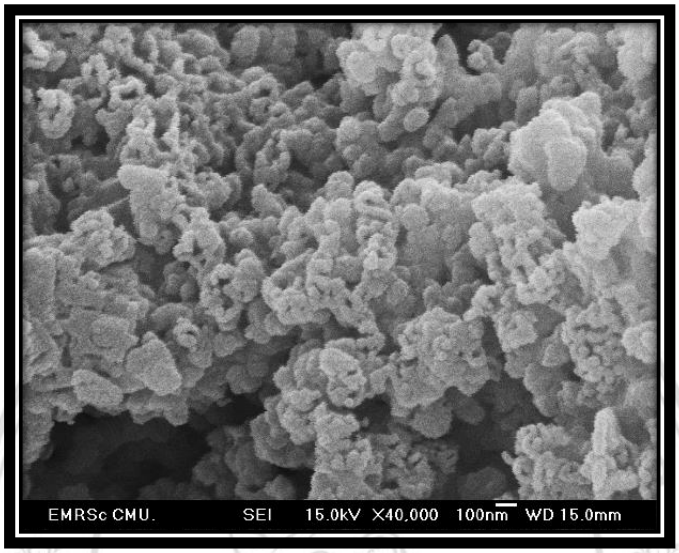

Figure 17. SEM images of CaO_2 when adding ascorbic acid.

Whereas SEM images of CaO_2 when adding ascorbic acid , which is selected because ascorbic acid molecule can act as chelating agent and connect between each CaO_2 particle to separate nuclei of CaO_2 particle, showed small particle size of CaO_2 in nanoparticle, approximately 10-20 nm. However, porous network forming was observed instead of nano dispersion shown in Fig 17.

Since the synthesized CaO_2 showed different morphology, morphology of commercial minor phases of $CaOH_2$ and $CaCO_3$ were investigated for minor phase comparison shown in Fig 18. and Fig 19. Below.

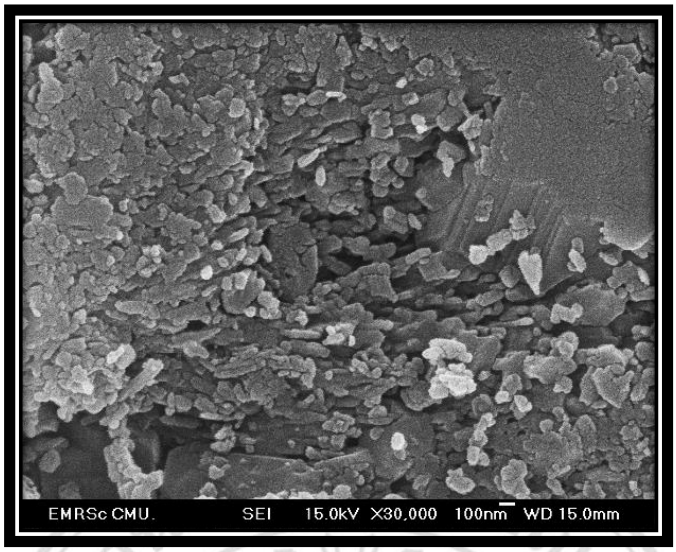

Figure 18. SEM images of $Ca(OH)_2$ commercial.

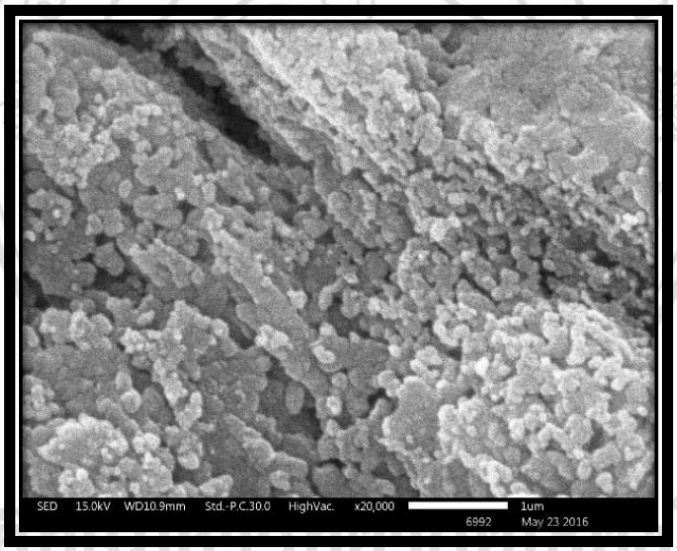

Figure 19. SEM images of $CaCO_3$commercial.

Fig 18. showed SEM image of commercial $Ca(OH)_2$, which is one of the minor phase of synthesized CaO_2 powders. It was found that particle looks similar to a big stone of dense CaO_2 with some bars being spread out. Whereas, commercial $CaCO_3$ Fig 19. particle has a spherical shape linking with others to a long network. Commercial $CaCO_3$ and $Ca(OH)_2$ morphology were different to the synthesized CaO_2.

3.8 Characterization of the CaO_2 powders by Transmission electron microscopy (TEM)

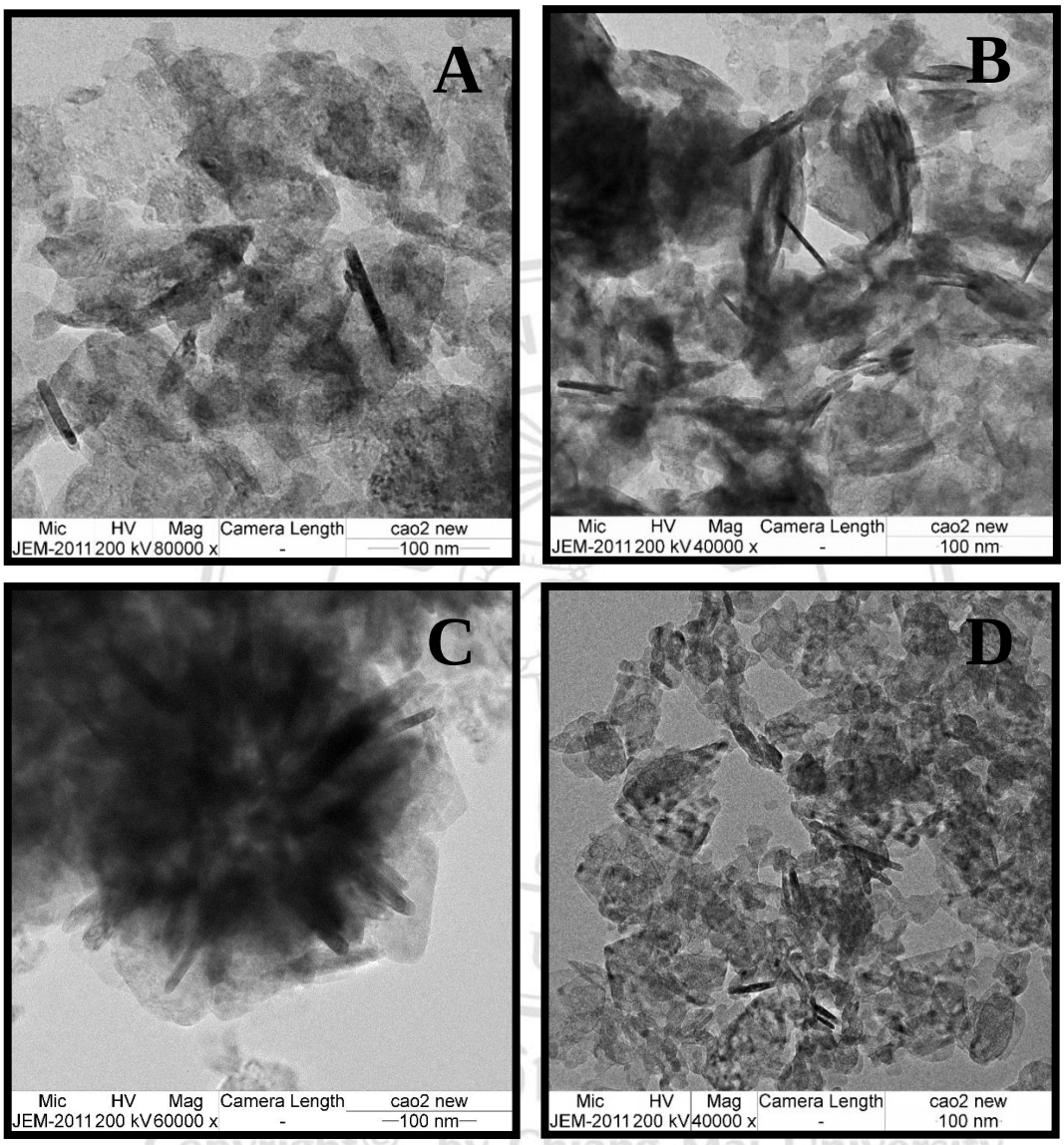

Figure 20. TEM images of the shape of CaO_2 mixing of mostly spherical and small amount of rod were obtained for the high purity CaO_2 powders.

Transmission electron microscopy (TEM) technique was used to reveal morphology of the particles. It can be confirmed that mixing of mostly spherical and small amount of rod shape was obtained for the high purity CaO_2 powders as shown in Fig 20. However, rod shape seems to be CaO_2 as well because composition of C:O ratio at the rod shape particle using EDS is consistent to CaO_2, not a minor phase $CaCO_3$. The spherical to rod shape transformation still need further investigation.

The best condition for synthesis of high purity CaO_2 nanoparticle can be obtained by using $Ca(NO_3)_2$ as a precursor and add H_2O_2 rapidly (Fig. 3.13). Then, adjust pH10 by NH_4OH and washed powders several times using NH_4OH. Finally, dried CaO_2 powders at 80°C for 2 hr. This condition provides CaO_2 in major phase and show $CaCO_3$ as small minor phase. Yellowish powders will be obtained after drying. Spherical particle, approximately 10-20 nm with some rod shape were observed by EM images.

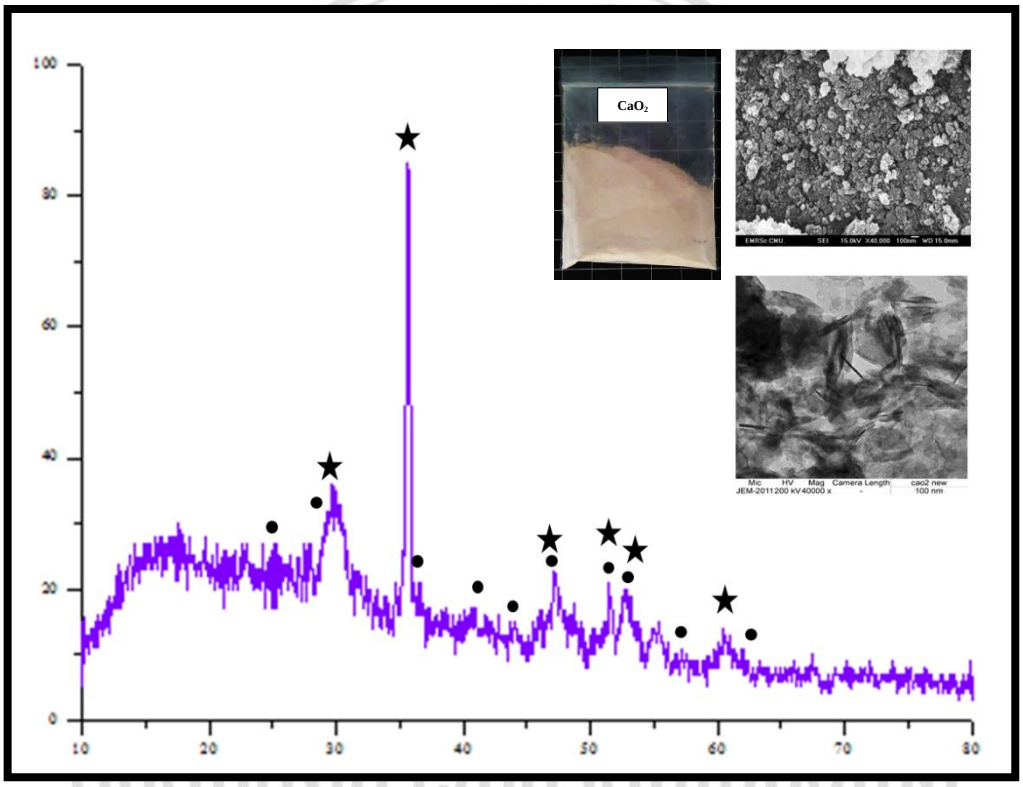

Figure 21. The best condition in synthesis of high purity CaO_2 nanoparticle.

3.9 The Brunauer–Emmett–Teller (BET) results

The BET method is the most widely used procedure for the determination of the surface area of solid materials and involves the use of the BET equation

$$v = \frac{v_m cp}{(p_0 - p)\{1 + (c-1)\left(\frac{p}{p_0}\right)\}}$$

Nanosized CaO_2 has a surface area of 13.16 m^2/g, which is rather large surface area compared to previous reports. Larger surface area is important for oxygen releasing and catalytic activities.

3.10 Disinfection of the synthesized CaO_2 powders.

Since CaO_2 will be dissolved in water and behave as hydrogen peroxide, disinfection was performed in this work. *S.aureus* and *E.coli*, which is adjusted to a turbidity of 0.5 McFarland, was swabbed on an NA plate. Antibacterial activity was investigated by measuring the zone of inhibition (clear zone).

Table 2. Disinfection of S.aureus and E.coli showing clear zone around calcium compounds

Chemical	*S.aureus*	*E.coli*
CaO_2 powders	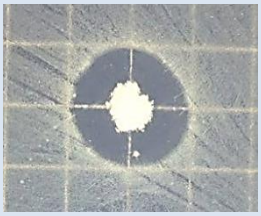	
$CaCO_3$ powders		

It was found that clear zone of *Staphylococcus aureus (S.aureus)* and *Escherichia coli (E. coli)* can be observed when using the synthesized CaO_2 powders, whereas no clear zone can be observed when using commercial $CaCO_3$. As a result, major phase CaO_2 is believed to active for bacteria disinfection.CaO_2 powders can inhibit growth of bacteria for both *E. coli* and *S. aureus*. The clear zone of CaO_2 powders were measuring approximately 6 mm.

3.11 UV -Vis diffuse reflectance spectrum of the CaO_2 powders

UV-Vis diffuse reflectance spectrum of CaO_2 powders was validated in order to utilize as a photocatalytic properties, for the first time to the best of our knowledge.

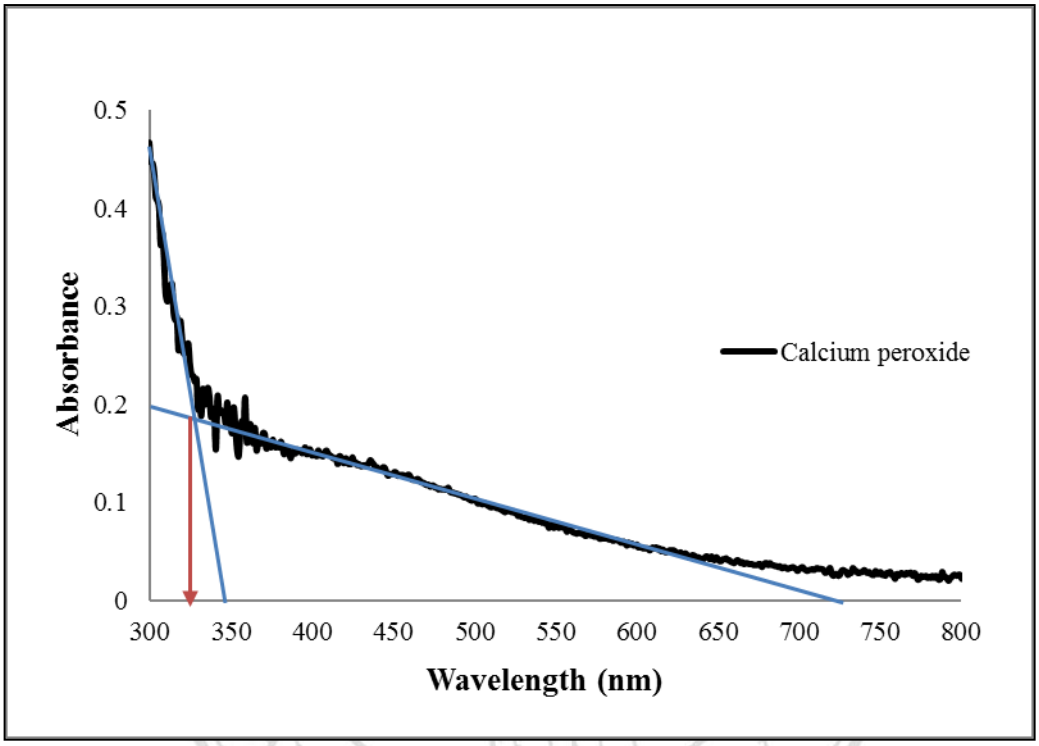

Figure 22. UV -Vis diffuse reflectance spectrum of the CaO_2 powders

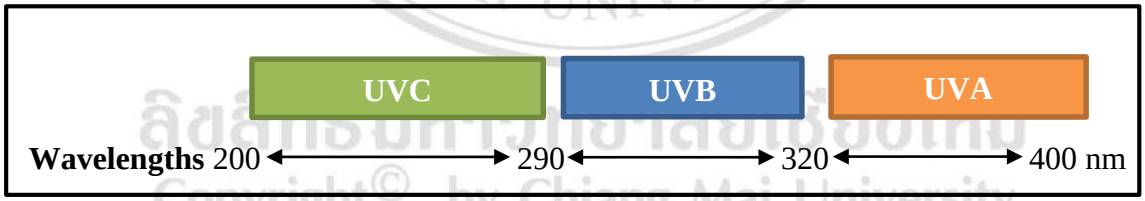

Figure 23. Wavelength of UVA, UVB and UVC

Fig 22. showed UV -Vis diffuse reflectance spectrum of the CaO_2 powders synthesized using $Ca(NO_3)_2$ with quickly addition of H_2O_2 and dried at 80°C. It was found that an absorption edge at approximately 330 nm or 3.75 eV was observed. The broad peak absorption at 400–550 nm or 3.1–2.25 eV also occurred. CaO_2 may show activity of photocatalyst under UV and visible light because of that absorption peaks.

3.12 Photocatalytic activity of CaO_2 powders under UVA, UVB and visible light

Fig 24. shows absorption overlap of CaO_2 powders and methylene blue solution in visible light (400-800 nm). Monitoring of photobleaching of methylene blue was chosen for photooxidation activity of CaO_2 powders investigation. It was found that CaO_2 can bleach methylene blue under UVA, UVB and visible light. No photoactivity was observed under dark condition and without CaO_2 as catalyst. Photosensitization of methylene blue was neglected as can be seen in Fig 24. because small amount of maximum wavelength of methylene blue solution was absorbed by the CaO_2.

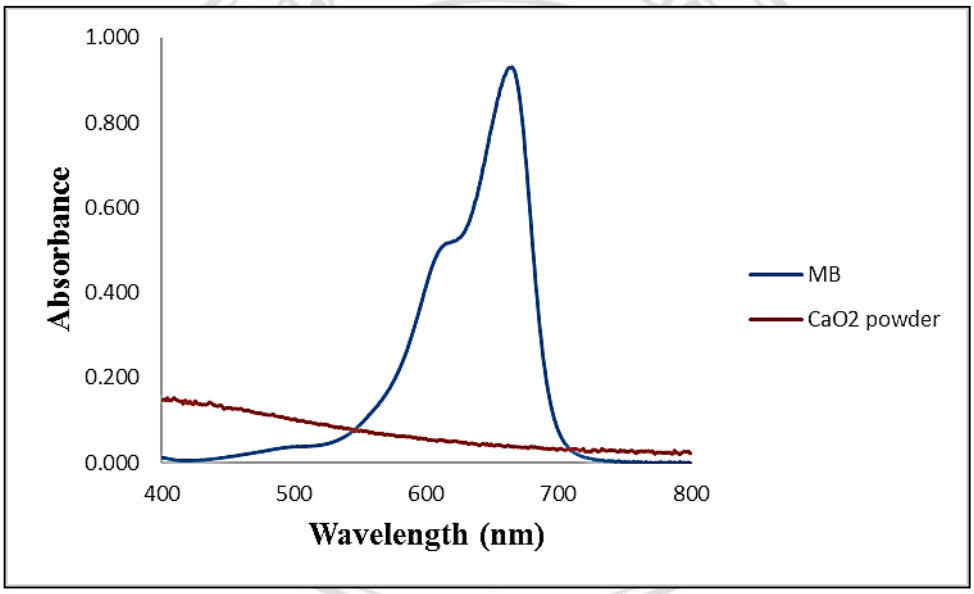

Figure 24. Light absorption overlapping of CaO_2 powders and methylene blue solution in visible light (400-800 nm).

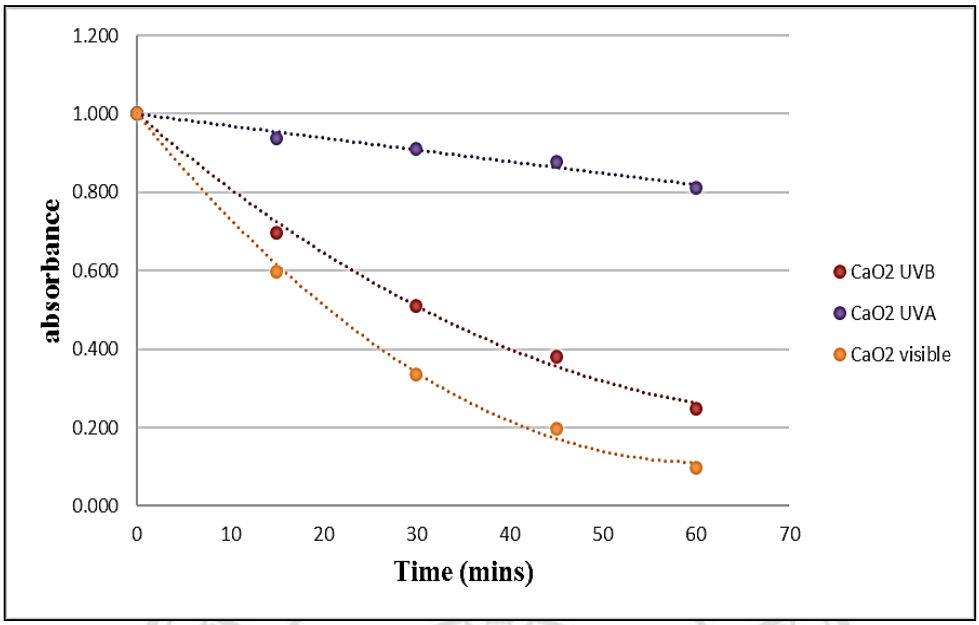

Figure 25. Photocatalytic activity of CaO_2 with different irradiation.

|Light source affected to photoactivity significantly as shown in Fig 25., which UVB, UVA and visible light from a homemade LED bulb reactor were compared. CaO_2 have the best performance of bleaching under visible light , probably because of CaO_2 absorb broad range of visible light as mentioned in Fig 24., UVB was absorbed higher than UVA consisting to the bleaching of methylene blue. However, as sunlight composed of UVA up to 5%, and visible approximately 45-50%, rarely UVB, the further experiments were focus on UVA and visible light. It is noteworthy that methylene blue was rapidly bleached when using CaO_2 as photocatalyst under visible light and can be reused for several times.

3.13 Photocatalytic activity of CaO_2 compared to $Ca(OH)_2$, $CaCO_3$ powders and H_2O_2 solution under UVA and visible light

To clarify the effect of CaO_2 on photobleaching of methylene blue, commercial $Ca(OH)_2$, $CaCO_3$ powders and H_2O_2 solution under UVA (Fig 26.), and visible light (Fig 27.) were also validated.

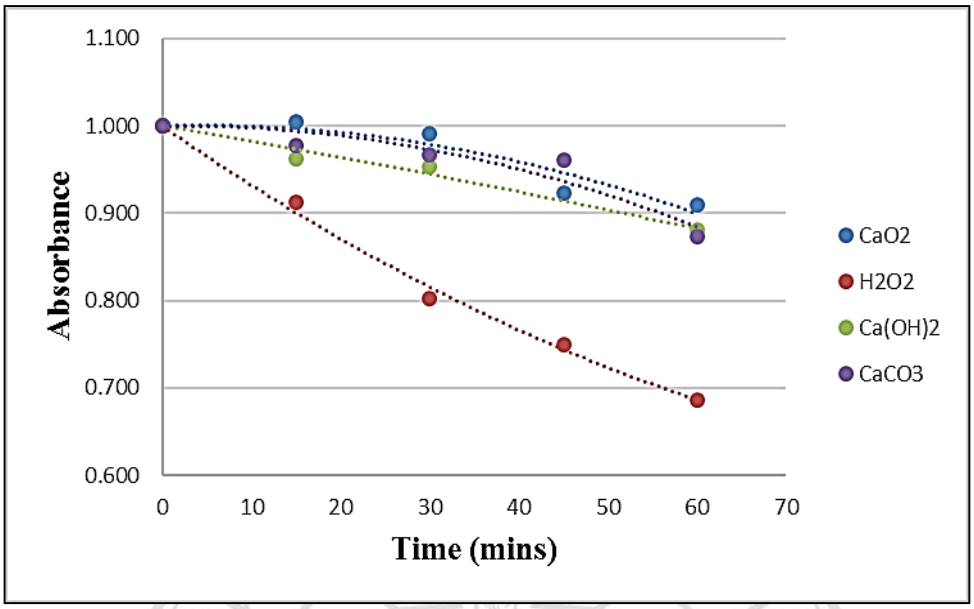

Figure 26. Photocatalytic activity of CaO_2 with UVA light in an hour.

Fig 26. showed bleaching of methylene blue solution when using CaO_2, $Ca(OH)_2$, $CaCO_3$ and H_2O_2 as catalyst. $CaCO_3$, $Ca(OH)_2$ and CaO_2 powders almost inactive under UVA and rarely bleaching of methylene blue can be observed. H_2O_2 showed promising photoactivity on bleaching methylene blue, due to H_2O_2 can generate hydroxyl radical from photodissociation of H_2O_2 under UVA. $^{\cdot}OH$ will oxidize methylene blue, resulting in reduction of absorbance rapidly. CaO_2 has a sharp absorption edge at 330 nm might be too high for the UVA bulb, which gives off 365 nm radiation, resulting in no activity of CaO_2 under UVA.

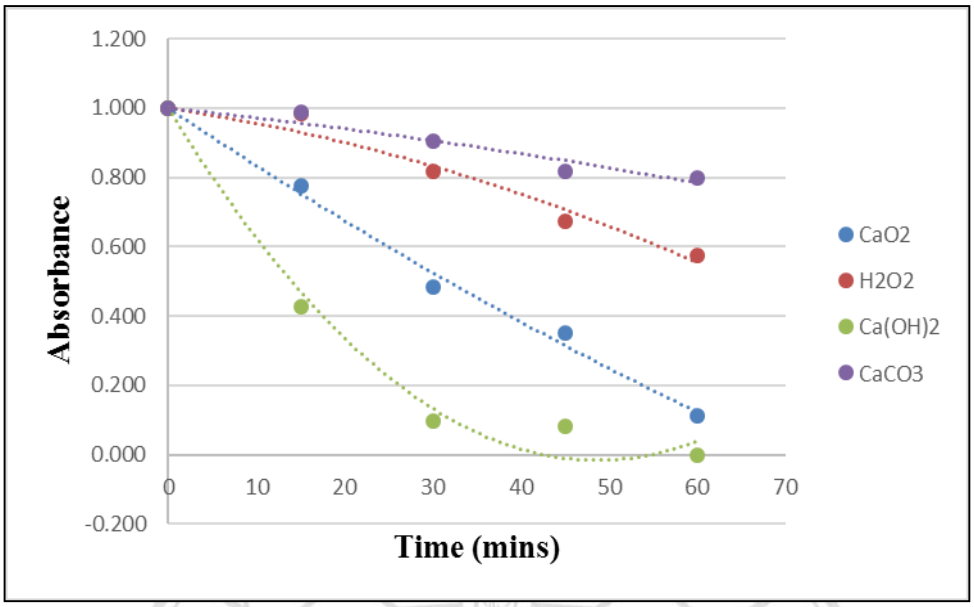

Figure 27. Photocatalytic activity of CaO_2 with UVB light in an hour.

Fig 27. showed decreasing absorbance of methylene blue under visible light. Contrary to photoactivity under UVA, $Ca(OH)_2$, CaO_2 exhibited good photoactivity on bleaching methylene blue than H_2O_2 because $Ca(OH)_2$ show broad peak absorption edge at 400-500 nm as well as broad peak of CaO_2 at 400–550 nm. As a result, $Ca(OH)_2$ and CaO_2 can be showed activity of photocatalyst under visible light. Whereas H_2O_2 showed less photoactivity than $Ca(OH)_2$, CaO_2 and also H_2O_2 under UVA because photodissociation of H_2O_2 was not complete occurred under visible light.

3.14 Photocatalytic activity of CaO_2 mixed with additive under visible light

Previously, additives affected to morphology of CaO_2 without affecting to phase transformation. It is interesting to find out the effect of additive to photoactivity. Photoactivity of CaO_2 synthesized by mixing with additive such as ethanol and ascorbic acid was performed under visible light as shown in Fig 28.

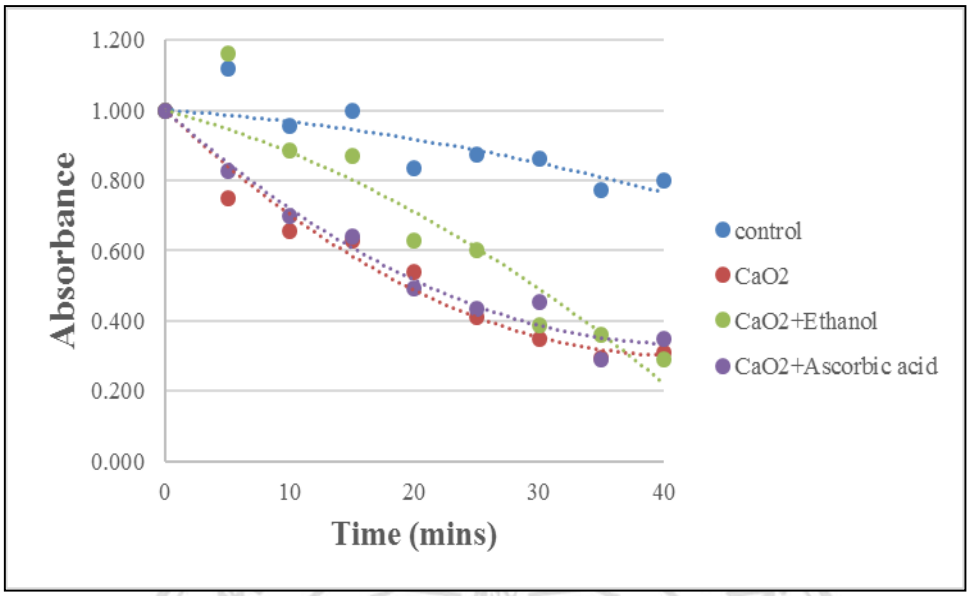

Figure 28. Photocatalytic activity of CaO_2 with visible light in an hour.

Fig 28. showed decreasing absorbance of methylene blue using CaO_2 mixed with additive as photocatalysts. It was found that non additive synthesized CaO_2 and CaO_2 mixed with ethanol, ascorbic acid presents the similar photoactivity under visible light.

3.15 Photoreduction of CaO_2, $CaCO_3$ and H_2O_2 determinate by Resazurin

In addition to photooxidative of CaO_2, its photoreduction of resazurin was measured and compared to $CaCO_3$ and H_2O_2. Results were shown in Table 3. below.

Table 3. Photoreduction of CaO_2, $CaCO_3$ and H_2O_2 in visible and UV light.

Chemicals	Begin	Final (UV light)	Final (visible light)
CaO_2		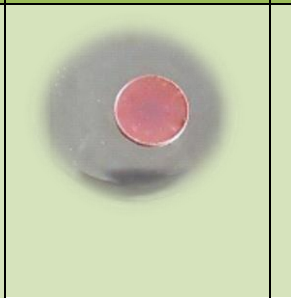	

Table 3. Photoreduction of CaO_2, $CaCO_3$ and H_2O_2 in visible and UV light. (Continued)

Chemicals	Begin	Final (UV light)	Final (visible light)
$CaCO_3$	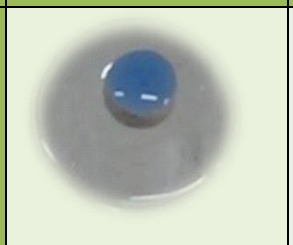		
H_2O_2		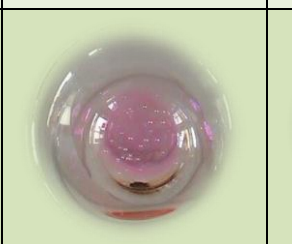	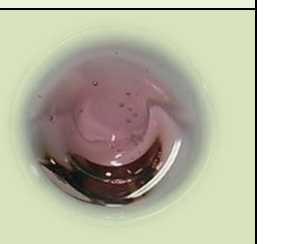

This table showed color change of resazurin from blue (resazurin) to pink (resorufin). It indicated a photoreduction activity of CaO_2 and H_2O_2 both under visible light and UV light within 5 mins. But no activity can be observed from $CaCO_3$, confirming the activity of CaO_2 major phase, not from minor phase.

In addition, CaO2 can be reused to reduce resazurin several times as shown in Table 4.

Table 4. Repeatability of photoreduction of CaO_2 in UV light.

Begin	Repeat#1	Repeat#2	Repeat#3	Repeat#4
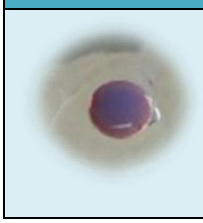	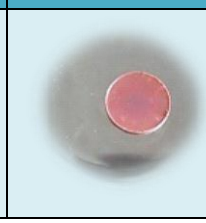			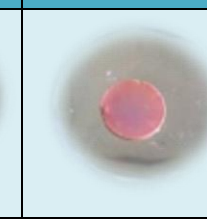

3.16 Oxygen releasing

Preliminary results of oxygen releasing of synthesized CaO_2 were shown in Table 5.

Table 5. Volume of oxygen in oxygen releasing of CaO_2 varying pH.

Days	pH 4 (ml)	pH 5 (ml)	pH6 (ml)
1	0.90	1.00	0.60
2	1.15	1.15	1.20
3	0.05	0.45	0.55
4	0.20	0.30	0.25
5	0.15	0.20	0.05
6	0.02	0.00	0.05
7	0.00	0.00	0.00

Oxygen releasing of CaO_2 powders showed inconsistency to pH and duration, probably due to some leakage of the instrumental set up. As a result, this preliminary results lack of reliable and need to be repeated with instrumental adaptation.